

High CO₂/CH₄ and C₂ Hydrocarbons/CH₄ Selectivity in a Chemically Robust Porous Coordination Polymer

Jingui Duan, Masakazu Higuchi, Satoshi Horike, Maw Lin Foo, Koya Prabhakara Rao, Yasutaka Inubushi, Tomohiro Fukushima, and Susumu Kitagawa*

A new porous coordination polymer, ([La(BTB)H₂O]·solvent (1Dguest)), is synthesized. Gas adsorption, ideal adsorbed solution theory (IAST) and breakthrough experiments of it exhibits high CH₄ separation capability toward CO₂ and C₂ hydrocarbons at 273 K. In addition, this also shows good water and chemical stability, in particular, it is stable at pH = 14 at 100 °C, which is unprecedented for carboxylate-based porous coordination polymers. Furthermore, the effective adsorption site for separation is revealed by using an in situ diffuse reflectance IR fourier transform (DRIFT) spectra study.

separation;^[4] however, until now, this is still a significant challenge.^[5] Traditionally, light hydrocarbon separations are performed by cryogenic distillation, which entails large energy costs.

Recently, a new class of designable and robust porous materials, porous coordination polymers (PCPs) or metal organic frameworks (MOFs),^[6] have demonstrated significant promise for adsorption and separation because of their chemical tailorability, which results in high BET surface areas and specific recognition ability

for components in the gas mixture.^[7]

Because of the theoretically limitless possibilities in assembling organic linkers and metal or cluster connectors, a large number of structures have been reported, but only a few of them show outstanding selectivity for CO₂ over CH₄,^[5] which is mainly attributed to the large quadrupole moment of CO₂ whereas CH₄ has none.^[8] In addition, the separation of C₂ (C₂H₄ and C₂H₆) from CH₄ mixtures has rarely been studied despite these light hydrocarbons being widely utilized as gas energy sources and raw materials.^[9] This is mainly due to their similar physical and chemical properties (kinetic parameters for C₂H₆: 3.9 Å; C₂H₄: 3.9 Å and CH₄: 3.8 Å), which lead to the difficulty for adsorption-based separation.^[10] However, among these few structures, their rather low hydrothermal and chemical stabilities, compared with zeolites, further limit their usage in moist and chemical environments. Therefore, candidate PCPs with high separation capability and enhanced stability in air, water, and acidic and basic media for methane separation are urgently needed.^[11]

In this light, several strategies have been employed to design frameworks with good water stability and high separation capability as follows. 1) Frameworks with dense open metal sites, such as MOF-74,^[6h,8] have good separation capacity, but frameworks with divalent metals are very sensitive to water and are even worse in acidic and basic environments. 2) Carborane-based frameworks with small pores and open metal sites show the predicted selectivity^[12], however, the stability of these frameworks has not yet been demonstrated. 3) Tetravalent metal-based frameworks, such as UiO-66,^[13] show good water stability, however, the 12-coordinated nodes may impede efficient adsorption sites.^[13] Therefore, even now, there is still no clear solution.

To overcome these issues, our strategy is to employ the trivalent La³⁺ ion and H₃BTB ligand (H₃BTB = 1,3,5-tris(4-carboxyphenyl)benzene) to construct porous frameworks. Because of

1. Introduction

Methane, with the highest heat of combustion per mass unit (55.7 kJ/g), is poised to be one of the most important energy source candidates in the future.^[1] However, geochemical gas streams commonly contain high concentrations of CO₂ and C₂ (C₂H₄ and C₂H₆) hydrocarbons that will result in the corrosion of gas pipelines^[2] and also impede the conversion of methane to value-added products.^[3] Thus, extensive efforts are being made worldwide for the development of efficient and economical

Dr. J. Duan, Dr. M. Higuchi, Dr. K. P. Rao,
Prof. S. Kitagawa
Institute for Integrated Cell-Material
Sciences (WPI-iCeMS)
Kyoto University
Yoshida, Sakyo-ku, Kyoto 606-8501, Japan
E-mail: kitagawa@icems.kyoto-u.ac.jp



Dr. S. Horike, T. Fukushima, Prof. S. Kitagawa
Department of Synthetic Chemistry and Biological Chemistry
Graduate School of Engineering
Kyoto University

Katsura, Nishikyo-ku, Kyoto 615-8510, Japan

Dr. M. L. Foo, Prof. S. Kitagawa
Japan Science and Technology Agency
ERATO, Kitagawa Integrated Pores Project
Kyoto Research Park
Bldg no. 3, Shimogogyo-ku, Kyoto 600-8815, Japan

Prof. S. Kitagawa
Japan Science and Technology Agency
ACT-C, Yoshida, Sakyo-ku
Kyoto 606-8501, Japan

Y. Inubushi
Synthesis Research Laboratory
Kurashiki Research Center
Kuraray Co. Ltd., 2045-1, Sakazu, Kurashiki, Okayama 710-0801, Japan

DOI: 10.1002/adfm.201203288

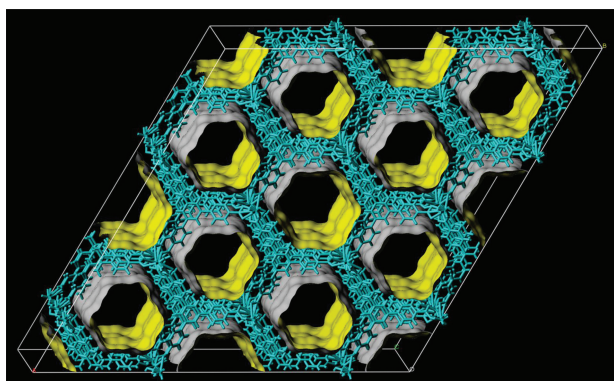


Figure 1. The Connolly surface diagram showing uniform 1-D channel in **1**. (Inner surfaces: yellow, outer surfaces: grey).

the high coordination number and large charge density (Z/r) of La^{3+} and with a rigid ligand, a triangular coordination connection may enhance the stability of the framework. Meanwhile, the large open metal site generated from the largest radius ion (La^{3+}) among all of the metals and uniform 1D channel may play positive roles in the adsorption-based separation. Here, we report the synthesis and structure of LaBTB (**Figure 1**), which is similar to MIL-103 (TbBTB),^[14] and that exhibits not only good CO_2/CH_4 and C_2 hydrocarbons/ CH_4 separation capability, but also unprecedented water and chemical stability.

2. Results and Discussion

2.1. Preparation, Characterization and Structure of $[\text{La}(\text{BTB})\text{H}_2\text{O}] \cdot \text{solvent} (1 \supset \text{guest})$

The new PCP, $[\text{La}(\text{BTB})\text{H}_2\text{O}] \cdot \text{solvent} (1 \supset \text{guest})$, was hydrothermally synthesized by a new method, different from previously reported,^[14] from a mixture of H_3BTB and $\text{La}(\text{NO}_3)_3 \cdot 6\text{H}_2\text{O}$ in N,N' -dimethylformamide/methanol/ H_2O . The structure was determined by single-crystal X-ray diffraction analysis, and the phase purity of the powder materials was confirmed by the powder X-ray diffraction pattern (PXRD) and elemental analysis. Thermogravimetric analysis (TGA) shows that **1** is thermally stable up to 350°C under N_2 atmosphere. After exchanging the guest solvents with methanol, we obtained the completely activated framework, as indicated by the IR and TG profiles (see the Supporting Information).

X-ray crystallography shows that **1** (Figure 1 and Supporting Information Figure S4–7) crystallizes in the $R32$ space group, $a = 28.764(4) \text{ \AA}$, $c = 12.563(3) \text{ \AA}$. We note that although powder diffraction patterns of LaBTB have been reported, no single crystal structure has been reported yet.^[14] The overall structure of **1** possesses 1D hexagonal channels (the size of the aperture window is ca. 10 \AA) with an open La chain. Because of the face-to-face assembly of the BTB ligands, the distances between the adjacent benzene rings vary from 3.53 to 4.47 \AA . In other words, between the two adjacent benzene rings, there is not enough space for the guest molecules, including even H_2 with the smallest molecular dimension. Thus, the well-packed benzene

rings with a high concentration of protons acts like a wall that can provide a hydrophobic environment for water stability.^[15] In addition, the accessible volume of the fully desolvated **1** is ca. 52.3% , calculated using the PLATON program^[16]. The total specific pore volume calculated from the maximum amount of N_2 adsorbed is $0.416 \text{ cm}^3 \text{ g}^{-1}$.

2.2. Water and Chemical Stability

Water and chemical stability are an important properties for any sorbent that has the potential to be used in so many important applications,^[17] especially for industry. However, the stability of PCP materials varies depending on the structure and the strength of the coordination bonds between metal clusters and ligands.^[18] The water and chemical stability of **1** were examined by soaking the as-synthesized samples in harsh conditions: hot (60°C and 100°C) aqueous HCl ($\text{pH} = 2$), aqueous NaOH ($\text{pH} = 14$) and water solutions for three days. The PXRD patterns of a series of samples strongly indicate the integrity of the framework under these conditions (**Figure 2**). Taking the crystal structure into consideration, the high water and chemical stability of **1** can be assigned to the combination of high coordination number, hydrophobic proton surface, face-to-face assembly of the rigid ligand units, triangular ligand unit and coordination type. To our knowledge, because of the relatively weak metal oxygen coordination, only a few carboxylate-bridged PCPs (MIL-100 series and UiO-66)^[11a,19] show structural stability in water, but for no longer than 24 h at room temperature, however, none have been known to be stable in an acid ($\text{pH} = 2$) at 60°C and base ($\text{pH} = 14$) solution at 60°C or 100°C for three days. More interestingly, the enhanced base stability at $\text{pH} = 14$ is unprecedented for carboxylate PCPs, although it has been observed before for zeolitic imidazole frameworks (ZIF-8^[17c]). Furthermore, to confirm the water streams stability, the evacuated framework was treated under 80°C , $80\% \text{ RH}$ and continued 24 h. The PXRD patterns also show the good integrity of **1**.

2.3. Gas Adsorption

To confirm the permanent porosity of **1**, the methanol-exchanged sample was degassed under high vacuum at 130°C

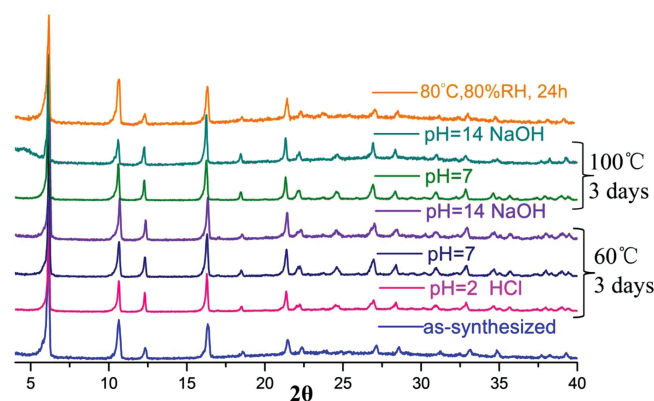


Figure 2. PXRD patterns of **1** after treatment.

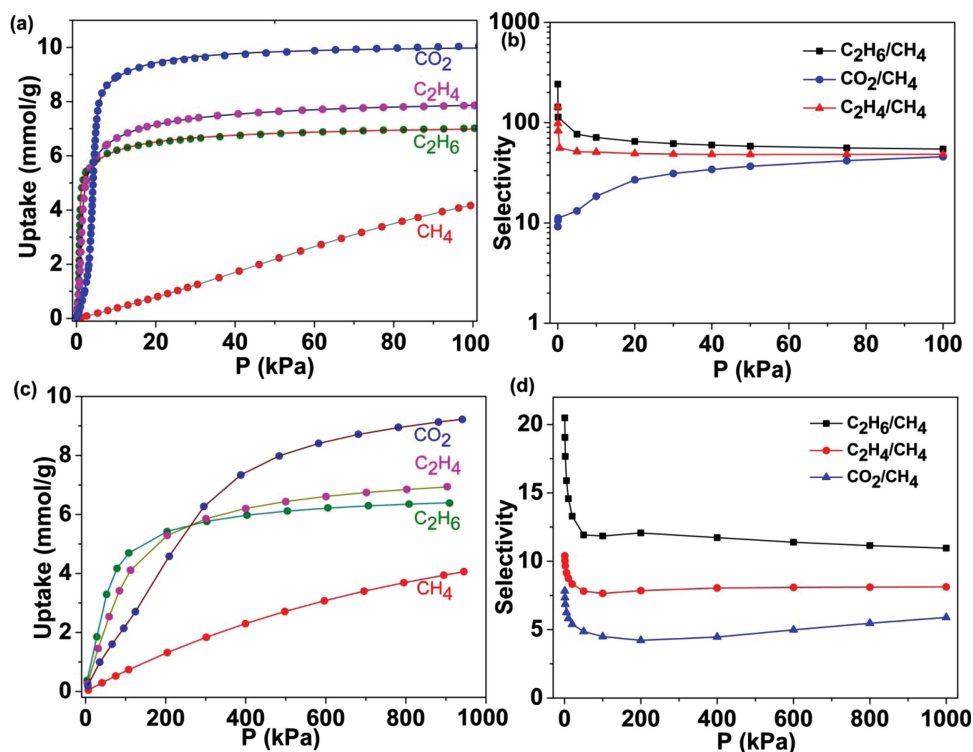


Figure 3. a,c) Gas adsorption isotherms (circle points) and the dual-site Langmuir–Freundlich fit curves (lines) for CO₂, CH₄, C₂H₄ and C₂H₆ in **1** at 195 K (100 kPa) and 273 K (1000 kPa), respectively. b,d) IAST predicted selectivity for C₂H₆/CH₄, C₂H₄/CH₄ and CO₂/CH₄ in **1**.

for 30 h to obtain the fully evacuated framework. N₂ adsorption for **1** at 77 K exhibited a reversible type-I isotherm, which is characteristic of microporous materials (Supporting Information Figure S8). The estimated apparent Brunauer–Emmett–Teller surface area (**1**: BET: $\approx 1024 \text{ m}^2 \text{ g}^{-1}$; Langmuir surface: $\approx 1136 \text{ m}^2 \text{ g}^{-1}$) is very close to the predicted theoretical value ($\approx 1080 \text{ m}^2 \text{ g}^{-1}$).^[20]

The uniform 1D channel with an open metal chain suggests that **1** might be a promising candidate for gas separation. Single-component adsorption isotherms for CH₄, CO₂, C₂H₄ and C₂H₆ were measured to 100 kPa at 195 K. As shown in Figure 3a, C₂H₄ and C₂H₆ adsorption isotherms in **1** display quick saturation around 10 kPa, however, the uptake of CH₄ increases slowly following this pressure. Importantly, the differences in the uptake amounts at $P = 10 \text{ kPa}$ (CO₂: 8.9 mmol/g; C₂H₆: 6.2 mmol/g; C₂H₄: 6.6 mmol/g; CH₄: 0.38 mmol/g) indicate that **1** is a potential candidate for the purification of CH₄ from C1 and C2 hydrocarbon mixtures. In addition, high-pressure measurements were performed at 273 K (Figure 3c), which confirmed the favorable adsorption of CO₂ and C2 hydrocarbons relative to CH₄. More interestingly, even though CO₂ has a large quadrupole moment, **1** prefers to capture the C2 hydrocarbons, which may be due to stronger electrostatic interactions between CO₂ molecules than that of C₂H₆.^[21]

In addition, more significant is the CO₂ adsorption capability of the evacuated **1** after humidity treatment at 80 °C, 80% RH continued for 24 h (Figure 4). Before the measurement, the humidity-treated sample was reactivated at 130 °C in vacuum for 20 h. The total uptake amount is almost the same (from

9.21 mmol/g to 8.53 mmol/g) which again strongly indicates the high water stability of **1**, even though in an extremely high moisture environment.

2.4. Ideal Adsorbed Solution Theory Simulation

Ideal adsorbed solution theory (IAST) is a precise method used to describe gas-mixture adsorption in representative zeolites

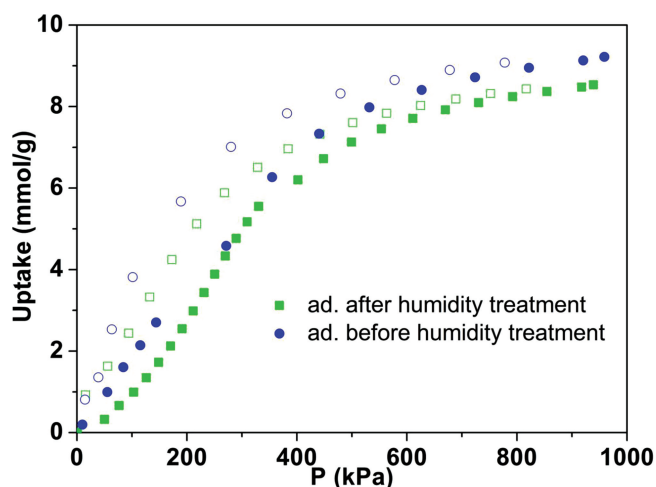


Figure 4. Comparison of CO₂ adsorption behaviors on evacuated **1** after/before humidity treatment.

and PCPs,^[22] and it was employed to predict multicomponent adsorption behaviors from the experimental single-component gas isotherms. The predicted adsorption selectivity for equimolar CO₂ and C₂ relative to CH₄ mixtures in **1** as a function of bulk pressure is presented in Figure 3b,d. As expected, the selectivity of C₂ relative to CH₄ has an unprecedented value (ca. 242–48) in the region of 100 kPa at 195 K. At 273 K, the predicted selectivity of C₂ to CH₄ (C₂H₆/CH₄: 22; C₂H₄/CH₄: 12) remains larger than 8, which indicates the practical feasibility of the procedure.^[23]

2.5. Breakthrough Experiments

To evaluate the gas separation ability for adsorbents, it is important to study not only a single gas component and IAST simulation under equilibrium conditions, but also under flowing (kinetic) conditions for a mixed gas.^[10] Thus, we proceeded to conduct breakthrough experiments, because they can evaluate the gas separation ability of adsorbents under kinetic flowing gas conditions, which are pertinent to the pressure swing adsorption (PSA) process used in industry.^[24] The breakthrough results for the CH₄ mixtures (CH₄/C₂H₆: 80/20; CH₄/CO₂: 60/40) in Figure 5 show that **1** has good capacity to purify CH₄. The concentration of outflowing gas by gas chromatography (GC) was almost 0% for C₂H₆ or CO₂ and 100% for CH₄, indicating that compound **1** provides complete separation of C₂H₆ or CO₂ from CH₄ under flowing conditions, which is consistent with equilibrium adsorption behaviors and the IAST results. Although there are so many other factors that can influence the retention time, it was obvious to see that the retention time for CH₄ in the mixtures is sufficient for the PSA process. Thus, because complete separation is achieved, **1** is a good candidate to purify CH₄ under both equilibrium and flow conditions.

2.6. In Situ DRIFT Spectra Studies

To understand the effect of the open metal site in **1**, we obtained in situ DRIFT spectra of CO₂ adsorption at 273 K with increasing pressure. Figure 6 presents the pressure-dependent IR absorption spectra. The band around 2300–2380 cm⁻¹, can be readily assigned to the ν₃ mode of CO₂ forming La³⁺...O=C=O adducts with end-on configuration.^[25] The band due to the ν₃ mode of CO₂ is similar to previous observations in HKUST-1^[25b] and CPO-27-Ni^[25a]. Therefore, the exposed La³⁺ site in **1** acts as a positive site for CO₂ capture. In addition, in the high frequency region (3800–3500 cm⁻¹), four components are observed at 3580, 3620, 3700, and 3730 cm⁻¹. The nature of these four absorptions is well known and can be assigned as the combination of ν₁ and ν₃ modes of CO₂. On the low frequency side (Supporting Information Figure S11), the νM-O mode of CO₂ can be clearly seen, showing that the molecule is weakly perturbed and also might be slightly distorted.^[25]

In addition, because the intensities of the C-H stretching bands (2900–3050 cm⁻¹) are a more sensitive indication of the perturbation of ethane adsorbed on open metal sites than the corresponding shifts of the stretching bands to lower frequencies^[26], from Supporting Information Figure S12, the apparent adsorption site, corresponding to the open coordination site of

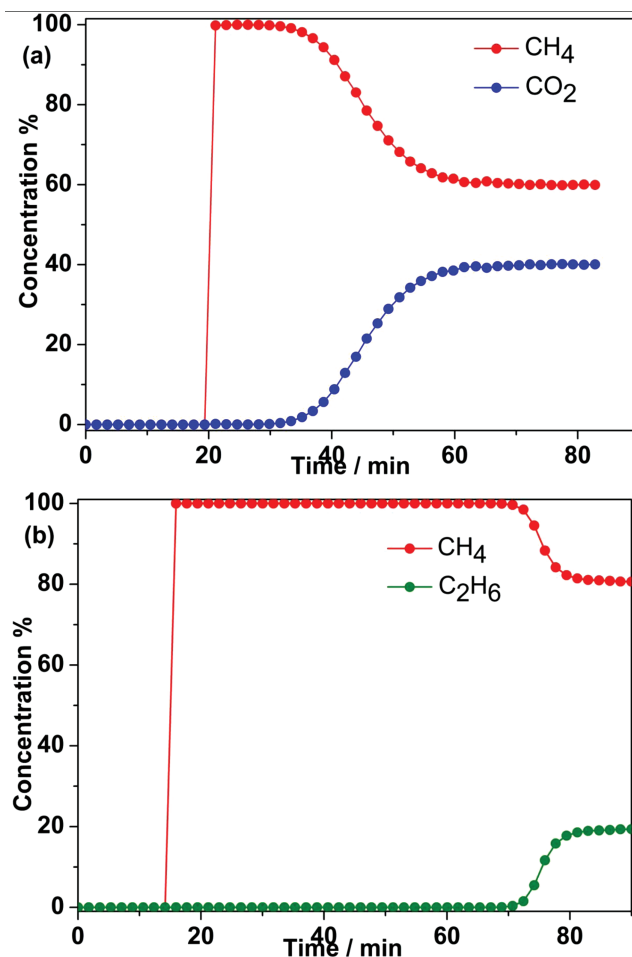


Figure 5. Breakthrough curves for a mixture of a) CH₄/CO₂ (60:40 v/v) and b) CH₄/C₂H₆ (80:20 v/v) on **1** at 0.8 MPa with 6 min⁻¹ space velocity at 273 K.

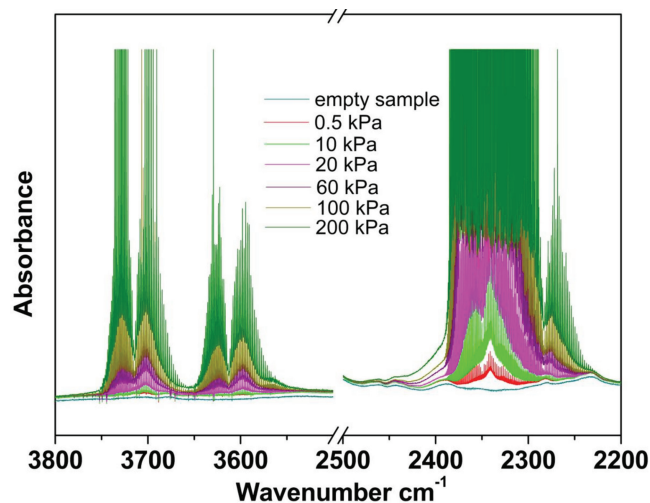


Figure 6. In situ DRIFT spectra (background subtracted) of CO₂ adsorbed on **1** at increasing equilibrium pressures.

the exposed La^{3+} cations was found, and C_2H_6 may display the side-on binding modes, similar to Fe-MOF-74 behavior.^[27]

3. Conclusion

In summary, we have synthesized a lanthanum-based PCP, $([\text{La}(\text{BTB})\text{H}_2\text{O}]\cdot\text{solvent} (1\text{-guest}))$, containing a 1-D hexagonal channel, open metal site and rich aromatic-proton organic wall. Adsorption experiments, IAST simulations and breakthrough experiments of **1** exhibit the excellent CH_4 purification capability from CO_2 or C_2 hydrocarbon mixtures. In addition, the in situ DRIFT spectra of adsorbed CO_2 and C_2H_6 provide the direct proof of the positive sites for separation. More interestingly, the high water and chemical stability of **1** will pave the way for practical usage for methane purification in the future.

4. Experimental Section

Materials: All the reagents and solvents were commercially available and used as received. The FTIR spectra were recorded in the range of $4000\text{--}400\text{ cm}^{-1}$ on a Nicolet ID5 ATR spectrometer. Thermal analyses were performed on a Rigaku TG8120 instruments from room temperature to $600\text{ }^\circ\text{C}$ at a heating rate of $5\text{ }^\circ\text{C}/\text{min}$ under flowing nitrogen. Powder X-ray diffraction was obtained using a Rigaku RINT powder diffractometer with $\text{Cu K}\alpha$ anode.

Synthesis of $[\text{La}(\text{BTB})\text{H}_2\text{O}]\cdot\text{Guest}$ (1-Guest): $\text{La}(\text{NO}_3)_3\cdot 6\text{H}_2\text{O}$ (17.6 mg, 0.040 mmol) and 1,3,5-tris(4-carboxyphenyl)benzene (H_3BTB , 6 mg, 0.0136 mmol) were mixed with 2 mL of $\text{DMF}/\text{MeOH}/\text{H}_2\text{O}$ (3:3:0.5) in a glass container and tightly capped with a Teflon vial and heated at $80\text{ }^\circ\text{C}$ for two days. After cooling to room temperature, colourless needle crystals were obtained. Yield: 63% (based on the ligand). Anal.Calc. for evacuated sample of **1** ($\text{C}_{27}\text{H}_{15}\text{LaO}_6$): C, 56.47; H, 2.63; Found: C, 56.81; H, 2.53. FTIR of as-synthesized samples (cm^{-1}): 3398 (s), 1650 (s), 1607 (s), 1579 (s), 1509 (s), 1386 (s), 1253 (s), 1185 (s), 1143 (s), 1098 (s), 1061 (s), 1017 (s), 934 (s), 850 (s), 780 (s), 706 (s), 661 (s), 595 (s).

Single Crystal X-Ray Study: The single crystal X-ray diffraction measurement was performed at 223 K with a Rigaku AFC10 diffractometer with Rigaku Saturn Kappa CCD system equipped with a MicroMax-007 HF/VariMax rotating-anode X-ray generator with confocal monochromated $\text{MoK}\alpha$ radiation. Data were processed using Crystal Clear TM-SM (Version 1.4.0). The structure was solved by direct methods and refined using the full-matrix least squares technique using the SHELXTL package.^[28] Nonhydrogen atoms were refined with anisotropic displacement parameters during the final cycles. Organic hydrogen atoms were placed in calculated positions with isotropic displacement parameters set to 1.2 Ueq of the attached atom. The unit cell includes a large region of disordered solvent molecules, which could not be modeled as discrete atomic sites. PLATON/SQUEEZE^[29] was employed to calculate the diffraction contribution of the solvent molecules and, thereby, to produce a set of solvent-free diffraction intensities; the structure was then refined again using the data generated.

Adsorption Experiments: Before the measurement, the solvent-exchanged sample (about 100 mg) was prepared by immersing the as-synthesized samples in methanol for three days to remove the nonvolatile solvents, and the extract was decanted every 8 h and fresh methanol was replaced. The completely activated sample was obtained by heating the solvent-exchanged sample at $130\text{ }^\circ\text{C}$ under a dynamic high vacuum for 30 h.

In the gas sorption measurement, ultrahigh-purity grade were used throughout the adsorption experiments. All of the measured sorption isotherms have been repeated twice to confirm the reproducibility within experimental error. Gas adsorption isotherms were obtained using a Belsorp-mini volumetric adsorption instrument from BEL Japan Inc. using the volumetric technique. To provide high accuracy and precision in

determining P/P_0 , the saturation pressure P_0 was measured throughout the N_2 analyses by means of a dedicated saturation pressure transducer, which allowed us to monitor the vapor pressure for each data point. A part of the N_2 sorption isotherm in the P/P_0 range 0.001–0.1 was fitted to the BET equation to estimate the BET surface area and the Langmuir surface area calculation was performed using all data points.

Breakthrough Measurements: Breakthrough curve measurements were performed using a hand-made gas-flow system. The sample cell was filled with 10 mL evacuated sample via large scale synthesis. The temperature of the cell was controlled by a circulating refrigerant system. For the CH_4/CO_2 mixture gas, the gas fraction was $\text{CH}_4:\text{CO}_2 = 60:40$ (v/v) with a pressure of 0.80 MPa. The experiments were performed at 273 K with a space velocity of 3 min^{-1} . For the $\text{CH}_4/\text{C}_2\text{H}_6$, the gas fraction was $\text{CH}_4:\text{C}_2\text{H}_6 = 80:20$ (v/v) with a pressure of 0.80 MPa. The experiments were performed at 273 K with a space velocity of 3 min^{-1} . The flow rates of all of the pure gases were regulated by mass flow controllers ($0\text{--}100\text{ mL}/\text{min}$). The gas stream at the outlet of the column was analyzed on-line with a GC.

Selectivity Prediction for Binary Mixture Adsorption: Ideal adsorbed solution theory (IAST)^[22] was used to predict binary mixture adsorption from the experimental pure-gas isotherms. To perform the integrations required by IAST, the single-component isotherms should be fitted by a proper model. There is no restriction on the choice of the model to fit the adsorption isotherm, however, data over the pressure range under study should be fitted very precisely.^[30] Several isotherm models were tested to fit the experimental pure isotherms for CH_4 , C_2H_4 , C_2H_6 and CO_2 of **1**, and the dual-site Langmuir–Freundlich equation were found to be the best fit to the experimental data:

$$q = q_{m1} \frac{b_1 P^{1/n_1}}{1 + b_1 P^{1/n_1}} + q_{m2} \frac{b_2 P^{1/n_2}}{1 + b_2 P^{1/n_2}} \quad (1)$$

Here, P is the pressure of the bulk gas at equilibrium with the adsorbed phase (kPa), q is the adsorbed amount per mass of adsorbent (mol/kg), q_{m1} and q_{m2} are the saturation capacities of sites 1 and 2 (mol/kg), b_1 and b_2 are the affinity coefficients of the sites ($1/\text{kPa}$), and n_1 and n_2 are measures of the deviations from an ideal homogeneous surface. Figure 3 shows that the dual-site Langmuir–Freundlich equation fits the single-component isotherms extremely well. The R_2 values for all of the fitted isotherms were over 0.99997. Hence, the fitted isotherm parameters were applied to perform the necessary integrations in IAST.

Crystal Data: $\text{C}_{27}\text{H}_{16}\text{LaO}_7$, $M_r = 591.31$, R_{32} , $a = 28.764(4)\text{ \AA}$, $c = 12.563(3)\text{ \AA}$, $V = 9001(3)\text{ \AA}^3$, $Z = 9$, $D_c = 0.982\text{ g}\cdot\text{cm}^{-3}$, $F_{000} = 2619$, $T = 223\text{ K}$, 21 154 reflections collected, 3746 independent reflections. After using the SQUEEZE command, $R_1 = 0.0424$, $wR_2 = 0.1152$ for $[I > 2\sigma(I)]$. CCDC: 904974.

Supporting Information

Supporting Information is available from the Wiley Online Library or from the author.

Acknowledgements

This work was supported by the Japan Society for the Promotion of Science (JSPS), ACT-C of the Japan Science and Technology Agency (JST), the New Energy and Industrial Technology Development Organization (NEDO), the JX Nippon Oil & Energy Corporation, and WPI iCeMS program. iCeMS is supported by the World Premier International Research Initiative (WPI) of MEXT, Japan.

Received: November 9, 2012
Published online: February 26, 2013

- [1] J. K. Stolaroff, S. Bhattacharyya, C. A. Smith, W. L. Bourcier, P. J. Cameron-Smith, R. D. Aines, *Environ. Sci. Technol.* **2012**, 46, 6455.
- [2] S. Cavenati, C. A. Grande, A. E. Rodrigues, *Energy Fuel* **2006**, 20, 2648.
- [3] V. R. Choudhary, S. Mayadevi, *Sep. Sci. Technol.* **1993**, 28, 2197.
- [4] C. A. Grande, S. Cavenati, F. A. Da Silva, A. E. Rodrigues, *Ind. Eng. Chem. Fundam.* **2005**, 44, 7218.
- [5] a) K. Sumida, D. L. Rogow, J. A. Mason, T. M. McDonald, E. D. Bloch, Z. R. Herm, T. H. Bae, J. R. Long, *Chem. Rev.* **2012**, 112, 724; b) J. R. Li, J. Sculley, H. C. Zhou, *Chem. Rev.* **2012**, 112, 869.
- [6] a) R. Matsuda, R. Kitaura, S. Kitagawa, Y. Kubota, R. V. Belosludov, T. C. Kobayashi, H. Sakamoto, T. Chiba, M. Takata, Y. Kawazoe, Y. Mita, *Nature* **2005**, 436, 238; b) H. Furukawa, N. Ko, Y. B. Go, N. Aratani, S. B. Choi, E. Choi, A. O. Yazaydin, R. Q. Snurr, M. O'Keeffe, J. Kim, O. M. Yaghi, *Science* **2010**, 329, 424; c) S. Q. Ma, D. F. Sun, J. M. Simmons, C. D. Collier, D. Q. Yuan, H. C. Zhou, *J. Am. Chem. Soc.* **2008**, 130, 1012; d) S. Kitagawa, R. Kitaura, S. Noro, *Angew. Chem. Int. Ed.* **2004**, 43, 2334; e) Y. Q. Lan, H. L. Jiang, S. L. Li, Q. Xu, *Adv. Mater.* **2011**, 23, 5015; f) J. R. Holst, A. I. Cooper, *Adv. Mater.* **2010**, 22, 5212; g) G. Ferey, C. Mellot-Draznieks, C. Serre, F. Millange, J. Dutour, S. Surble, I. Margiolaki, *Science* **2005**, 309, 2040; h) Y. S. Bae, C. Y. Lee, K. C. Kim, O. K. Farha, P. Nickias, J. T. Hupp, S. T. Nguyen, R. Q. Snurr, *Angew. Chem. Int. Ed.* **2012**, 51, 1857; i) L. J. Murray, M. Dinca, J. R. Long, *Chem. Soc. Rev.* **2009**, 38, 1294; j) J. Y. Lee, L. Pan, X. Y. Huang, T. J. Emge, J. Li, *Adv. Funct. Mater.* **2011**, 21, 993.
- [7] a) S. C. Xiang, W. Zhou, Z. J. Zhang, M. A. Green, Y. Liu, B. L. Chen, *Angew. Chem. Int. Ed.* **2010**, 49, 4615; b) Z. R. Herm, R. Krishna, J. R. Long, *Microporous Mesoporous Mater.* **2012**, 151, 481.
- [8] D. Britt, H. Furukawa, B. Wang, T. G. Glover, O. M. Yaghi, *Proc. Natl. Acad. Sci. USA* **2009**, 106, 20637.
- [9] Y. B. He, Z. J. Zhang, S. C. Xiang, F. R. Fronczek, R. Krishna, B. L. Chen, *Chem. Eur. J.* **2012**, 18, 613.
- [10] S. Horike, K. Kishida, Y. Watanabe, Y. Inubushi, D. Umeyama, M. Sugimoto, T. Fukushima, M. Inukai, S. Kitagawa, *J. Am. Chem. Soc.* **2012**, 134, 9852.
- [11] a) K. A. Cychoz, A. J. Matzger, *Langmuir* **2010**, 26, 17198; b) S. J. Yang, C. R. Park, *Adv. Mater.* **2012**, 24, 4010.
- [12] Y. S. Bae, O. K. Farha, A. M. Spokoyny, C. A. Mirkin, J. T. Hupp, R. Q. Snurr, *Chem. Commun.* **2008**, 4135.
- [13] J. H. Cavka, S. Jakobsen, U. Olsbye, N. Guillou, C. Lamberti, S. Bordiga, K. P. Lillerud, *J. Am. Chem. Soc.* **2008**, 130, 13850.
- [14] T. Devic, C. Serre, N. Audebrand, J. Marrot, G. Ferey, *J. Am. Chem. Soc.* **2005**, 127, 12788.
- [15] L. Pan, B. Parker, X. Y. Huang, D. H. Olson, J. Lee, J. Li, *J. Am. Chem. Soc.* **2006**, 128, 4180.
- [16] A. L. Spek, PLATON, A Multipurpose Crystallographic Tool, Utrecht University, The Netherlands, 2001.
- [17] a) V. Colombo, S. Galli, H. J. Choi, G. D. Han, A. Maspero, G. Palmisano, N. Masciocchi, J. R. Long, *Chem. Sci.* **2011**, 2, 1311; b) H. J. Choi, M. Dinca, A. Dailly, J. R. Long, *Energy Environ. Sci.* **2010**, 3, 117; c) K. S. Park, Z. Ni, A. P. Cote, J. Y. Choi, R. D. Huang, F. J. Uribe-Romo, H. K. Chae, M. O'Keeffe, O. M. Yaghi, *Proc. Natl. Acad. Sci. USA* **2006**, 103, 10186.
- [18] a) J. J. Low, A. I. Benin, P. Jakubczak, J. F. Abrahamian, S. A. Faheem, R. R. Willis, *J. Am. Chem. Soc.* **2009**, 131, 15834; b) I. J. Kang, N. A. Khan, E. Haque, S. H. Jhung, *Chem. Eur. J.* **2011**, 17, 6437.
- [19] M. Kandiah, M. H. Nilsen, S. Usseglio, S. Jakobsen, U. Olsbye, M. Tilset, C. Larabi, E. A. Quadrelli, F. Bonino, K. P. Lillerud, *Chem. Mater.* **2010**, 22, 6632.
- [20] J. G. Duan, Z. Yang, J. F. Bai, B. S. Zheng, Y. Z. Li, S. H. Li, *Chem. Commun.* **2012**, 48, 3058.
- [21] K. S. Walton, A. R. Millward, D. Dubbeldam, H. Frost, J. J. Low, O. M. Yaghi, R. Q. Snurr, *J. Am. Chem. Soc.* **2008**, 130, 406.
- [22] a) Y. S. Bae, K. L. Mulfort, H. Frost, P. Ryan, S. Punathanam, L. J. Broadbelt, J. T. Hupp, R. Q. Snurr, *Langmuir* **2008**, 24, 8592; b) N. F. Cessford, N. A. Seaton, T. Duren, *Ind. Eng. Chem. Res.* **2012**, 51, 4911.
- [23] Y. B. He, Z. J. Zhang, S. C. Xiang, F. R. Fronczek, R. Krishna, B. L. Chen, *Chem. Commun.* **2012**, 48, 6493.
- [24] M. L. Foo, S. Horike, Y. Inubushi, S. Kitagawa, *Angew. Chem. Int. Ed.* **2012**, 51, 6107.
- [25] a) P. D. C. Dietzel, R. E. Johnsen, H. Fjellvag, S. Bordiga, E. Groppo, S. Chavan, R. Blom, *Chem. Commun.* **2008**, 5125; b) S. Bordiga, L. Regli, F. Bonino, E. Groppo, C. Lamberti, B. Xiao, P. S. Wheatley, R. E. Morris, A. Zecchina, *Phys. Chem. Chem. Phys.* **2007**, 9, 2676.
- [26] V. B. Kazansky, I. R. Subbotina, F. C. Jentoft, R. Schlogl, *J. Phys. Chem. B* **2006**, 110, 17468.
- [27] E. D. Bloch, W. L. Queen, R. Krishna, J. M. Zadrozny, C. M. Brown, J. R. Long, *Science* **2012**, 335, 1606.
- [28] G. M. Sheldrick, *Acta Crystallogr. Sect. A* **2008**, 64, 112.
- [29] a) A. L. Spek, *J. Appl. Crystallogr.* **2003**, 36, 7; b) P. Vandersluis, A. L. Spek, *Acta Crystallogr. Sect. A* **1990**, 46, 194.
- [30] a) R. Babarao, Z. Q. Hu, J. W. Jiang, S. Chempath, S. I. Sandler, *Langmuir* **2007**, 23, 659; b) V. Goetz, O. Pupier, A. Guillot, *Adsorption* **2006**, 12, 55.